Nonplanar Distortion Modes for Highly Substituted Porphyrins

Craig J. Medforth,† Mathias O. Senge,† Kevin M. Smith,*,† Laurie D. Sparks,‡ and John A. Shelnutt*,‡

Contribution from the Department of Chemistry, University of California, Davis, California 95616, and Fuel Science Department 6211, Sandia National Laboratories, Albuquerque, New Mexico 87185. *Received April 8, 1992. Revised Manuscript Received August 3, 1992*

Abstract: The syntheses, structures, and spectroscopic properties of some novel dodecaphenyl- and dodecaalkylporphyrins have been investigated with the aim of designing model compounds to aid in evaluating theoretical models of porphyrin nonplanarity. It was found that dodecaphenylporphyrin (**3**) and the dodecaalkylporphyrins **4a–c** could be prepared using standard synthetic procedures and that these porphyrins adopted very distorted nonplanar structures in the crystalline state. In the crystal structure of **3** the pyrrole rings were tilted with respect to the mean plane of the porphyrin to give a saddle conformation, whereas in the crystal structure of the nickel(II) complex of **4c** (Ni**4c**) the pyrrole rings were twisted with respect to the mean plane to give a ruffled conformation. Nonplanar conformations with the same distortion modes were obtained as minimum energy structures for Ni**3** and Ni**4c** using a molecular mechanics force field, which showed that the observed nonplanar conformations were due to steric repulsions between the peripheral substituents. Low-temperature NMR spectra indicated that the solution conformations of **3** and Ni**4c** were consistent with those found in the crystal structures. Several conformations of Ni**4b** and Ni**4c** with different quasi-axial and quasi-equatorial orientations of the alkyl chains were observed in solution, and saddle and ruffled distortion modes were clearly differentiated for the dications and nickel(II) complexes of porphyrins **4b** and **4c**. Finally, an attempt was made to synthesize the dodecaalkylporphyrin **5** using the same conditions applied to porphyrins **4a–c**. This gave only the 5,15-dihydroporphyrin **6**, presumably because the more spatially demanding six-membered ring prevented the oxidation of **6** to porphyrin **5** using 2,3-dichloro-5,6-dicyano-1,4-benzoquinone.

Introduction

There exists a large body of structural data which shows that the porphyrin macrocycle is conformationally flexible and capable of adopting nonplanar conformations.[1,2] This conformational flexibility has recently become a topic of interest because of the role it may play in controlling the biological properties of tetrapyrroles in systems as diverse as photosynthetic reaction centers,[3] photosynthetic antenna systems,[4] factor F_{430} from methylreductase,[5] vitamin B_{12} and B_{12}-dependent enzymes,[6] and heme proteins.[7] Several studies[8-13] have explored the effects of nonplanarity on the porphyrin macrocycle using highly substituted porphyrins such as those shown in Figure 1. These investigations have shown that some of the effects seen in nonplanar model compounds (e.g., changes in redox potentials, optical absorption spectra, and spin delocalization) can be related to biological systems. For example, INDO/s calculations indicate that the series of absorption maxima seen for the bacteriochlorophylls in the antenna complex of *Prosthecochloris aestuarii* in a low-temperature glass can be partially explained by differences in the conformations of the individual chlorophylls.[14]

This growing recognition of the importance of porphyrin conformational flexibility prompted us to investigate some of the ways in which different substituents affect the structural and spectroscopic properties of highly substituted porphyrins. We prepared porphyrins **2a–c** (see Figure 1) in which varying degrees of steric crowding were introduced at the periphery of the porphyrin to produce macrocycles with different degrees of nonplanarity.[11,12] This approach utilized the ability of progressively larger alkano rings to increase the unfavorable peripheral steric interactions that are responsible for a nonplanar conformation. These porphyrins were investigated by X-ray crystallography, molecular mechanics calculations, visible spectrophotometry, and resonance Raman and NMR spectroscopy, and the spectroscopic results were correlated with the nonplanarity of the macrocycle.[11,12,15]

In the present work, we investigate the possibility of varying the peripheral substituents of highly substituted porphyrins to produce macrocycles which distort from planarity in different ways. These compounds promise to be useful models for investigating the effects of nonplanarity on the porphyrin macrocycle and for evaluating theoretical models of porphyrin nonplanarity.

In the course of our investigations we have synthesized dodecaphenylporphyrin[16-18] (**3**) and the first dodecaalkylporphyrins[20]

† University of California.
‡ Sandia National Laboratories.

(1) (a) Hoard, J. L. In *Porphyrins and Metalloporphyrins*; Smith, K. M., Ed.; Elsevier: Amsterdam, **1975**; Chapter 8. (b) Scheidt, W. R. In *The Porphyrins*; Dolphin, D., Ed.; Academic Press: New York, **1979**; Vol. 3, Chapter 10.

(2) Scheidt, W. R.; Lee Y. J. *Struct. Bonding (Berlin)* **1987**, *64*, 1.

(3) (a) Deisenhofer, J.; Michel, H. *Angew. Chem., Int. Ed. Engl.* **1989**, *28*, 829. (b) Deisenhofer, J.; Michel, H. *Science* **1989**, *245*, 1463.

(4) Trourud, D. E.; Schmid, M. F.; Matthews, B. W. *J. Mol. Biol.* **1986**, *188*, 443.

(5) (a) Furenlid, L. R.; Renner, M. W.; Smith, K. M.; Fajer, J. *J. Am. Chem. Soc.* **1990**, *112*, 1634. (b) Furenlid, L. R.; Renner, M. W.; Fajer, J. *J. Am. Chem. Soc.* **1990**, *112*, 8987.

(6) Geno, M. K.; Halpern, J. *J. Am. Chem. Soc.* **1987**, *109*, 1238.

(7) Alden, R. G.; Ondrias, M. R.; Shelnutt, J. A. *J. Am. Chem. Soc.* **1990**, *112*, 691.

(8) Barkigia, K. M.; Chantranupong, L.; Smith, K. M.; Fajer, J. *J. Am. Chem. Soc.* **1988**, *110*, 7566.

(9) Barkigia, K. M.; Berber, M. D.; Fajer, J.; Medforth, C. J.; Renner, M. W.; Smith, K. M. *J. Am. Chem. Soc.* **1990**, *112*, 8851.

(10) Renner, M. W.; Cheng, R.-J.; Chang, C. K.; Fajer, J. *J. Phys. Chem.* **1990**, *94*, 8508.

(11) Medforth, C. J.; Berber, M. D.; Smith, K. M.; Shelnutt, J. A. *Tetrahedron Lett.* **1990**, *31*, 3719.

(12) Shelnutt, J. A.; Medforth, C. J.; Berber, M. D.; Barkigia, K. M.; Smith, K. M. *J. Am. Chem. Soc.* **1991**, *113*, 4077. The current force field uses an improper torsion term of the form $E_\omega = \Sigma\gamma_\omega (1 - \cos\omega_0)$ and a cutoff distance of 50 Å for nonbonded interactions.

(13) The use of highly substituted porphyrins in evaluating the effects of porphyrin nonplanarity in relation to biological systems has been described: (a) Fajer, J.; Barkigia, K. M.; Smith, K. M.; Zhong, E.; Gudowska-Nowak, E.; Newton, M. In *Reaction Centers of Photosynthetic Bacteria*; Michel-Beyerle, M. E., Ed.; Springer-Verlag: Berlin, **1990**, 367. (b) Fajer, J. *Chem. Ind. (London)* **1991**, 869.

(14) Gudowska-Nowak, E.; Newton, M. D.; Fajer, J. *J. Phys. Chem.* **1990**, *94*, 5795.

(15) Complete crystallographic data for porphyrins **1a–c** and **2b–d** will be reported elsewhere: (a) Barkigia, K. M.; Berber, M. D.; Fajer, J.; Furenlid, L. R.; Medforth, C. J.; Renner, M. W.; Smith, K. M. Manuscript in preparation. (b) Medforth, C. J.; Senge, M. O.; Smith, K. M.; Sparks, L. D.; Shelnutt, J. A. Submitted for publication.

(16) We have reported some details of the synthesis and solution conformation of dodecaphenylporphyrin in a communication: Medforth, C. J.; Smith, K. M. *Tetrahedron Lett.* **1990**, *31*, 5583.

(17) Optical spectra and a molecular mechanics calculation for the nickel(II) complex of dodecaphenylporphyrin have been briefly reported.[12]

(18) Syntheses and spectroscopic properties of some other dodecaarylporphyrins have been described.[19] A preliminary crystal structure of dodecaphenylporphyrin showing the macrocycle in a nonplanar conformation has been noted, but no details were given.[19b]

0002-7863/92/1514-9859$03.00/0

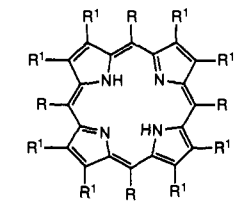

1a R = C_6H_5; R^1 = CH_3
1b R = C_6H_5; R^1 = CH_2CH_3
1c R = C_6H_5; R^1 = $CH_2CH_2CH_3$
3 R = R^1 = C_6H_5

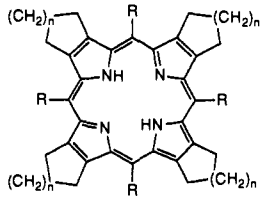

2a n = 1; R = C_6H_5
2b n = 2; R = C_6H_5
2c n = 3; R = C_6H_5
2d n = 1; R = (3,4,5-OCH_3)-C_6H_2
4a n = 1; R = CH_3
4b n = 1; R = CH_2CH_3
4c n = 1; R = $CH_2CH_2CH_2CH_2CH_3$
5 n = 2; R = CH_2CH_3

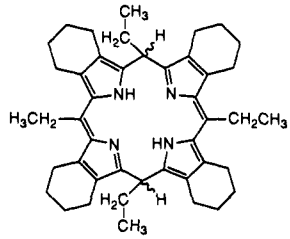

6

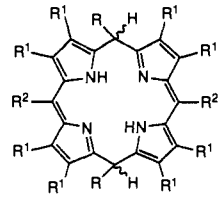

7 R = CH_3; R^1 = CH_2CH_3; R^2 = H
8 R = R^2 = C_6H_5; R^1 = CH_3

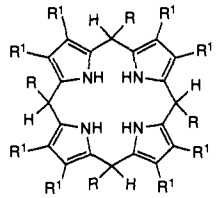

9 R = C_6H_5; R^1 = CH_3
10 R = C_6H_5; R^1 = CH_2CH_3

Figure 1. Molecular structures of some highly substituted porphyrins. Porphyrins **1a–c** and **2a–d** have been investigated previously.[8,9,11–13,15] Porphyrins **3** and **4a–c** are new compounds investigated in this study.

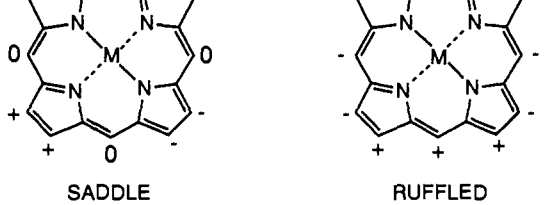

Figure 2. Idealized saddle and ruffled distortion modes for the porphyrin macrocycle using the nomenclature of Scheidt and Lee.[2] Displacements of the atoms with respect to the porphyrin least-squares plane are shown as + = above the plane, − = below the plane, and 0 = in the plane.

(**4a–c**). X-ray crystallography is used to show that **3** exists in a very nonplanar saddle conformation, whereas the nickel(II) complex of **4c** (**Ni4c**) exists in a very nonplanar ruffled conformation (idealized forms of these conformations are shown in Figure 2). The crystal structures are then compared to structures calculated using a molecular mechanics force field for nickel(II) porphyrins.[12,21] The solution conformations of the dodecasubstituted porphyrins are also investigated by low-temperature NMR spectroscopy.

Experimental Section

Syntheses of Porphyrins 3 and 4a–c. Dodecaphenylporphyrin and the dodecaalkylporphyrins were prepared using the procedure already described for porphyrins **1a** and **1b**.[9] This procedure is similar to that reported by Lindsey and co-workers for the synthesis of 5,10,15,20-tetraphenyl-21*H*,23*H*-porphine (TPP),[22] and it involves the $BF_3{\cdot}OEt_2$-catalyzed condensation of an aldehyde with a 3,4-disubstituted pyrrole and subsequent oxidation of the porphyrinogen using 2,3-dichloro-5,6-dicyano-1,4-benzoquinone (DDQ).

Benzaldehyde, acetaldehyde, propionaldehyde, and hexanal were obtained commercially (Aldrich) and used without further purification. 3,4-Diphenylpyrrole was prepared using the procedure described by Friedman.[23] The synthesis of the dimethyl *N*-acetyliminodiacetate precursor used in this reaction is not described in the original paper.[23] We prepared dimethyl *N*-acetyliminodiacetate from iminodiacetic acid (Aldrich). Hydrochloric acid gas was passed through a stirred suspension of iminodiacetic acid (6 g) in boiling methanol (20 mL) until a clear solution was obtained (1–2 h). This solution was neutralized with potassium carbonate solution and extracted several times with dichloromethane. After the dichloromethane was removed under vacuum, dimethyl iminodiacetate was obtained as a pale brown oil in 83% yield. Dimethyl *N*-acetyliminodiacetate was prepared by reacting this sample of dimethyl iminodiacetate with a 5-fold excess of acetic anhydride and then removing the acetic anhydride and acetic acid under high vacuum. This gave a thick oil, which was dissolved in a minimum volume of hot dichloromethane, and the dimethyl *N*-acetyliminodiacetate was crystallized by addition of diethyl ether. The yield of dimethyl *N*-acetyliminodiacetate was 71%. 3,4-Propanopyrrole was prepared in 43% yield by steam distillation of 3,4-propanopyrrole-2-carboxylic acid. The latter was obtained by hydrolyzing ethyl 3,4-propanopyrrole-2-carboxylate in refluxing 2 M KOH for 30 min, cooling the mixture in an ice bath, carefully neutralizing the solution with 2 M HCl, and then filtering off the resulting precipitate. Ethyl 3,4-propanopyrrole-2-carboxylate was prepared in 28% yield from 1-nitrocyclopentene[24] using the procedure described by Barton and Zard.[25]

Porphyrin **3** was purified by column chromatography using grade III neutral alumina and 40% dichloromethane in cyclohexane as eluent. This column gave the following fractions in order of elution: (1) a brown band, (2) a green band identified as the dication of **3** and (3) a blue band identified as containing largely 3,4-diphenylpyrrole. As the separation between bands 1 and 2 was not complete, the sample was passed through another column of grade III neutral alumina using toluene as eluent. This allowed complete separation of the brown and green bands. The toluene was removed under high vacuum and the porphyrin dication dissolved in a minimum volume of dichloromethane. Three drops of a solution of KOH (1 pellet) in ethanol (2 mL) was sufficient to form the free base porphyrin, whereupon addition of more ethanol caused the formation of green crystals. These crystals were filtered off and vacuum dried for 30 min at 70 °C, after which time the crystals had changed to a black powder, presumably due to loss of solvent. Porphyrins **4a–c** were typically purified by column chromatography using neutral grade III alumina with dichloromethane as eluent and were recrystallized from dichloromethane using the same procedure described for **3**. A progressive increase in solubility in organic solvents was noted for **4a–c** as the alkyl chain became longer. All of the dodecaalkylporphyrins were quite soluble in dichloromethane containing 1% trifluoroacetic acid. The yields (unoptimized) were as follows: **3**, 6%; **4a**, 16%; **4b**, 20%; and **4c**, 52%.

Nickel(II) porphyrins were prepared using the metal acetate method.[26] For **3** the metalation was incomplete after 2–3 days, so **Ni3** was purified by column chromatography using neutral grade III alumina with 20% dichloromethane in cyclohexane as eluent. **Ni3** eluted first as a red band, followed by a green band for the dication of **3**. The nickel(II) porphyrins were crystallized from dichloromethane by addition of methanol. A progressive increase in solubility with increasing alkyl chain length was noted for **Ni4a–c**.

Attempted Synthesis of Other Dodecaalkylporphyrins. Previous studies[11,12,15] have indicated that a fused six-membered ring (e.g., **2b**) causes a considerable increase in peripheral steric repulsions and nonplanarity when compared to a fused five-membered ring (e.g., **2a** or **2d**). An attempt was therefore made to prepare porphyrin **5** from the reaction of 3,4-butanopyrrole[11] with propionaldehyde.

An optical spectrum of the crude reaction mixture after oxidation with DDQ revealed a sharp band at approximately 460 nm and some other broad bands between 500 and 700 nm. The reaction mixture was purified

(19) (a) Tsuchiya, S. *Chem. Phys. Lett.* **1990**, *169*, 608. (b) Takeda, J.; Ohya, T.; Sato, M.; *Chem. Phys. Lett.* **1991**, *183*, 384. (c) Tsuchiya, S. *J. Chem. Soc., Chem. Commun.* **1991**, 716.

(20) A search of the literature did not reveal any syntheses or crystal structures of dodecaalkylporphyrins.

(21) Molecular mechanics calculations have recently been used to investigate the conformational flexibility of some hydroporphyrins, including factor F_{430}: (a) Kaplan, W. A.; Suslick, K. S.; Scott, R. A. *J. Am. Chem. Soc.* **1990**, *112*, 1283. (b) Kaplan, W. A.; Suslick, K. S.; Scott, R. A. *J. Am. Chem. Soc.* **1991**, *113*, 9824.

(22) Hsu, H. C.; Kearney, P. C.; Lindsey, J. S.; Margueretiaz, A. M.; Schreiman, I. C. *J. Org. Chem.* **1987**, *52*, 827.

(23) Friedman, M. *J. Org. Chem.* **1965**, *30*, 859.

(24) Corey, E. J.; Estreicher, H. *J. Am. Chem. Soc.* **1978**, *100*, 6294.

(25) Barton, D. H. R.; Zard, S. Z. *J. Chem. Soc., Chem. Commun.* **1985**, 1098.

(26) Buchler, J. W. In *Porphyrins and Metalloporphyrins*; Smith, K. M., Ed.; Elsevier: Amsterdam, **1975**; Chapter 5, page 179.

by column chromatography, and a reasonably pure sample of the product with a 460-nm absorption was obtained. The optical spectrum of this material in dichloromethane containing 1% trifluoroacetic acid consisted of essentially a single broad band at 460 nm. In dichloromethane without trifluoroacetic acid the absorption maximum was found at 432 nm.

A 300-MHz proton NMR spectrum in $CDCl_3$ revealed no signals upfield of TMS, indicating that the material was not a porphyrin. However, there was a broad singlet at approximately δ 15 which integrated to two hydrogens. The remainder of the spectrum consisted of an ethyl group [2.80 (q, 4 H, CH_2) and 1.19 (t, 6 H, CH_3)], a $CHCH_2CH_3$ group [3.70 (t, 2 H, CH), 2.29 (m, 4 H, CH_2), and 0.97 (t, 6H, CH_3)], and some butano protons [2.76 and 2.44 (m, 8 H each, ring $CH_2\alpha$), 1.72 (m, 16 H, ring $CH_2\beta$)]. A structure consistent with this optical and NMR data is the 5,15-dihydroporphyrin **6**. The signal at δ 15 must be due to the NH protons of the pyrrole rings. The related 5,15-dihydroporphyrin **7**[27] has a similar NH proton chemical shift (δ 12.58) and a similar visible absorption spectrum (single band at 420 nm in benzene). Based on structure **6** the yield was calculated to be 6%.

Ni**6** was prepared using the metal acetate method.[26] As expected, the signal at δ 15 was absent in the metalated material. The optical spectrum of Ni**6** showed bands at 438 and 544 nm compared to 435 and 541 nm for Ni**7**. The proton NMR spectrum of Ni**6** in CD_2Cl_2 at room temperature was slightly broadened, but in C_6D_6 at 343 K the lines were sharp and could be readily assigned: 3.77 (t, 2 H, $CHCH_2CH_3$), 3.14 (m, 4 H, $CHCH_2CH_3$), and 1.26 (t, 6 H, $CHCH_2CH_3$); 2.71 (q, 4 H, CH_2CH_3) and 1.10 (t, 6 H, CH_2CH_3); 2.63 and 2.38 (m, 8 H each, ring $CH_2\alpha$) and 1.59 (m, 16 H, ring $CH_2\beta$). Attempts to prepare crystals of Ni**6** suitable for a crystal structure determination were unsuccessful.

Other intermediates along the synthetic pathway to highly substituted porphyrins have been isolated.[28,29] Dolphin[28] isolated **8** and **9** as intermediates in the synthesis of porphyrin **1a**, and Smith, Evans, and Fuhrhop[29] have obtained **10** as an intermediate in the synthesis of porphyrin **1b**. In our case the intermediate **6** must be much more difficult to oxidize than the precursors to porphyrins **1a** and **1b**. The latter can be readily oxidized to the corresponding porphyrins with DDQ in refluxing dichloromethane, whereas **6** resists oxidation with DDQ even upon reflux in toluene.

In the light of these results it was not suprising that our attempts to prepare 2,3,5,7,8,10,12,13,15,17,18,20-dodecaethylporphyrin (from 3,4-diethylpyrrole and propionaldehyde) and 2,3,7,8,12,13,17,18-octaphenyl-5,10,15,20-tetraethylporphyrin (from 3,4-diphenylpyrrole and propionaldehyde) were unsuccessful.

Proton NMR Spectroscopy and Spectrophotometry. Proton NMR spectra were recorded at frequencies of 300 or 500 MHz. All chemical shifts are given in ppm and have been converted to the δ scale using the solvent peak at δ 5.30 for CD_2Cl_2 or CD_2Cl_2/CS_2 and δ 7.26 for $CDCl_3$ or $CDCl_3/CS_2$. Spectra were assigned with the aid of homonuclear decoupling and saturation transfer experiments. A magnitude-mode COSY spectrum of Ni**4b** was taken at 178 K using a standard software package.

Proton-decoupled carbon-13 spectra were recorded at a frequency of 75 MHz. All chemical shifts are given in ppm and have been converted to the δ scale using the solvent signal at δ 53.6 for CD_2Cl_2 or CD_2Cl_2/CS_2 and δ 77.0 for $CDCl_3$. The variable temperature unit was calibrated using a sample of methanol.[30]

Visible spectra absorption maxima (nm) and absorption coefficients ($\epsilon \times 10^{-3}$) were recorded on a Hewlett-Packard 8450A spectrophotometer using dichloromethane as solvent.

NMR Data for Precursors and Pyrroles. Dimethyl iminodiacetate: ($CDCl_3$) 2.04 (s, 1 H, NH), 3.46 (s, 4 H, CH_2), 3.72 (s, 6 H, CH_3).

Dimethyl *N*-acetyliminodiacetate: ($CDCl_3$) 4.20 and 4.15 (s, 2 H each, CH_2), 3.78 and 3.72 (s, 3 H each, CO_2CH_3), 2.12 (s, 3 H, CH_3CO). The CH_2 and CH_3 signals are doubled due to restricted rotation about the amide bond.

Ethyl 3,4-propanopyrrole-2-carboxylate: ($CDCl_3$) 8.76 (br, 1 H, NH), 6.59 (d, 1 H, H-pyrrole), 4.28 (q, 2 H, $CO_2CH_2CH_3$), 2.83 and 2.64 (t, 2 H each, ring $CH_2\alpha$), 2.35 (m, 2 H, ring $CH_2\beta$), 1.33 (t, 3 H, $CO_2CH_2CH_3$).

3,4-Propanopyrrole: ($CDCl_3$) 7.91 (br, 1 H, NH), 6.44 (d, 2 H, H-pyrrole), 2.65 (t, 4 H, ring $CH_2\alpha$), 2.33 (m, 2 H, ring $CH_2\beta$).

Optical and NMR Data for Porphyrins. 3: proton NMR (CD_2Cl_2) (298 K) 7.61 (d, 8 H, meso H_{ortho}), 6.73 (m, 52 H, remaining protons), −0.9 (br s, 2 H, NH); (193 K) 7.90, 7.44, 6.01, and 5.63 (d, 4 H each, pyrrole H_{ortho}), 6.96, 6.78, 6.47, and 6.44 (t, 4 H each, pyrrole H_{meta}), 6.73 and 6.64 (t, 4 H each, pyrrole H_{para}), 7.87 and 7.65 (d, 4 H each, meso H_{ortho}), 6.96 and 6.68 (t, 4 H each, meso H_{meta}), 6.78 (t, 4 H, meso H_{para}), −1.5 (br s, 2 H, NH); visible spectrum (CH_2Cl_2) λ_{max} ($\epsilon \times 10^{-3}$) 468 nm (238), 564 (14.3), 616 (15.0), 724 (9.0); proton NMR (CD_2Cl_2 plus 1% TFA) (299 K) 8.09 (d, 8 H, meso H_{ortho}), 7.12 (m, 12 H, meso $H_{meta/para}$), 6.71 (m, 40 H, pyrrole $H_{ortho/meta/para}$); (178 K) 8.19 (d, 8 H, meso H_{ortho}), 7.17 (t, 8 H, meso H_{meta}), 7.09 (t, 4 H, meso H_{para}), 7.97 and 5.30 (br, 8 H each, pyrrole H_{ortho}), 7.00 and 6.43 (br, 8 H each, pyrrole H_{meta}), 6.77 (t, 4 H, pyrrole H_{para}); visible spectrum (CH_2Cl_2 plus 1% TFA) λ_{max} ($\epsilon \times 10^{-3}$) 490 nm (225), 594 (sh), 646 (sh), 718 (46.7).

Ni**3**: proton NMR (CD_2Cl_2) 7.01 (d, 8 H, meso H_{ortho}), 6.51 (t, 8 H, meso H_{meta}), 6.65 (m, 44 H, remaining protons); carbon-13 NMR ($CDCl_3$) δ 148.2, 139.8, 137.2, 136.6, 134.0, 131.0, 126.5, 126.2, 125.1, 124.8, 119.9; visible spectrum (CH_2Cl_2) λ_{max} ($\epsilon \times 10^{-3}$) 448 nm (239), 566 (17.8) and 613 (19.0).

4a: proton NMR (CD_2Cl_2 plus 1% TFA) (293 K) 4.38 (s, 12 H, CH_3), 3.97 (t, 16 H, ring $CH_2\alpha$), 2.90 (m, 8 H, ring $CH_2\beta$), −3.07 (br s, 4 H, NH); (183 K) 4.32 (s, 12 H, CH_3), 4.32 and 3.56 (br m, 8 H each, ring $CH_2\alpha$), 3.07 and 2.52 (br m, 4 H each, ring $CH_2\beta$), −3.64 (s, 4 H, NH); visible spectrum (CH_2Cl_2 plus 1% TFA) λ_{max} ($\epsilon \times 10^{-3}$) 424 nm (413), 540 (4.2), 580 (15.1), 630 (24.1). The free base porphyrin was not sufficiently soluble to allow the measurement of a proton NMR spectrum.

Ni**4a**: proton NMR ($CDCl_3/CS_2$, 1:3) 3.74 (s, 12 H, CH_3), 3.90 (t, 16 H, ring $CH_2\alpha$), 2.97 (m, 8 H, ring $CH_2\beta$); visible spectrum (saturated solution in CH_2Cl_2) λ_{max} 418 nm, 540, 580.

4b: proton NMR ($CDCl_3$) 4.85 (q, 8 H, CH_2), 4.13 (br t, 16 H, ring $CH_2\alpha$), 3.08 (br m, 8 H, ring $CH_2\beta$), 1.82 (br t, 12 H, CH_3), −3.26 (br s, 2 H, NH); visible spectrum (CH_2Cl_2) λ_{max} ($\epsilon \times 10^{-3}$) 416 nm (318), 484 (4.4), 516 (21.3), 550 (7.1), 596 (5.7), 652 (7.7); proton NMR (CD_2Cl_2 plus 1% TFA) (293 K) 4.70 (q, 8 H, CH_2), 3.89 (br, 16 H, ring $CH_2\alpha$), 2.91 (br m, 8 H, ring $CH_2\beta$), 2.00 (t, 12 H, CH_3), −1.7 (br s, 4 H, NH); (193 K) 4.76 and 4.59 (br, 4 H each, CH_2), 4.27 and 3.54 (br, 8 H each, ring $CH_2\alpha$), 3.10 and 2.61 (br, 4 H each, ring $CH_2\beta$), 1.95 (br, 12 H, CH_3), −1.6 (br, 4 H, NH); visible spectrum (CH_2Cl_2 plus 1% TFA) λ_{max} ($\epsilon \times 10^{-3}$) 426 nm (433), 542 (4.2), 582 (14.8), 630 (28.9).

Ni**4b**: proton NMR (CD_2Cl_2/CS_2, 1:3) (293 K) 4.28 (q, 8 H, CH_2), 3.94 (t, 16 H, ring $CH_2\alpha$), 2.97 (m, 8 H, ring $CH_2\beta$), 1.22 (t, 12 H, CH_3); (174 K) 4.26 (q, CH_2), 4.02 and 3.75 (m, ring $CH_2\alpha$), 2.93 (m, 8 H, ring $CH_2\beta$), 1.08 (t, CH_3) (weighted average of six methyl signals at 2.22, 1.58, 1.54, 0.89, 0.85, and 0.80 ppm); visible spectrum (CH_2Cl_2) λ_{max} 420 nm, 544, 582.

4c: proton NMR ($CDCl_3$) 4.73 (br t, 8 H, α CH_2), 4.07 (br, 16 H, ring $CH_2\alpha$), 3.05 (m, 8 H, ring $CH_2\beta$), 2.07 (br, 8 H, βCH_2), 1.74 (br, 8 H, γCH_2), 1.50 (br m, 8 H, δCH_2), 0.97 (br t, 12 H, CH_3), −3.15 (br, 2 H, NH); carbon-13 NMR (CD_2Cl_2) (294 K) 117.6, 38.2, 34.4, 33.6, 32.5, 31.0, 23.9, 15.0; (213 K) 152.8, 146.9, 144.9, 130.1, 117.1, 38.3, 34.0, 33.4, 31.8, 30.8, 23.7, 14.9; visible spectrum (CH_2Cl_2) λ_{max} ($\epsilon \times 10^{-3}$) 416 nm (317), 484 (3.9), 518 (19.8), 552 (7.5), 598 (5.2), 654 (8.0); proton NMR (CD_2Cl_2 plus 1% TFA) (293 K) 4.60 (t, 8 H, αCH_2), 3.86 (br, 16 H, ring $CH_2\alpha$), 2.89 (br m, 8 H, ring $CH_2\beta$), 2.34 (br m, 8 H, βCH_2), 1.87 (m, 8 H, γCH_2), 1.60 (m, 8 H, δCH_2), 1.05 (t, 12 H, CH_3), −2.2 (br s, 4 H, NH); (183 K) 4.60 and 4.48 (br, 4 H each, αCH_2), 4.21 (br, 8 H, ring $CH_2\alpha$), 3.61 and 3.42 (br, 4 H each, ring $CH_2\alpha$), 3.07 (br, 4 H, ring $CH_2\beta$), 2.72 and 2.54 (br, 2 H each, ring $CH_2\beta$), 2.32 and 2.15 (br, 4 H each, βCH_2), 1.83 (br, 8 H, γCH_2), 1.49 (br, 8 H, δCH_2), 0.98 (br, 12 H, CH_3), −3.0 (br s, 4 H, NH); visible spectrum (CH_2Cl_2 plus 1% TFA) λ_{max} ($\epsilon \times 10^{-3}$) 428 nm (475), 544 (4.2), 584 (13.7), 632 (30.2).

Ni**4c**: proton NMR (CD_2Cl_2) (293 K) 4.29 (t, 8 H, αCH_2), 3.89 (br t, 16 H, ring $CH_2\alpha$), 2.91 (m, 8 H, ring $CH_2\beta$), 1.38 (br m, 8 H, βCH_2), 1.13 (br m, 16 H, γCH_2 and δCH_2), 0.67 (br t, 12 H, CH_3); (194 K) 4.26 (br t, 8 H, αCH_2), 4.00 and 3.68 (br m, ring $CH_2\alpha$), 2.85 (br m, 8 H, ring $CH_2\beta$), 1.38 (br m, 8 H, βCH_2) (weighted average of three methylene signals at 2.57, 1.83, and 1.05 ppm), 0.91 (br m, 16 H, γCH_2 and δCH_2), 0.48 (m, CH_3); carbon-13 NMR (CD_2Cl_2/CS_2, 1:3, 293 K, CS_2 = δ 192.3) 150.2, 133.6, 114.8, 34.7, 32.4, 32.2, 31.9, 30.3, 23.0, 14.2; visible spectrum (CH_2Cl_2) λ_{max} ($\epsilon \times 10^{-3}$) 422 nm (234), 546 (16.8), 582 (4.5).

Crystal Structure Determinations. Our initial aim was to obtain crystal structures for the nickel(II) complexes of the newly synthesized porphyrins so that a direct comparison would be possible with the minimum energy structures calculated using a molecular mechanics force field for nickel(II) porphyrins.[12] This proved to be more difficult than first anticipated, as Ni**4a** was not sufficiently soluble to be recrystallized, Ni**4b** did not crystallize well, and several crystallization techniques failed to produce suitable crystals of Ni**3**. Cobalt(II) and copper(II) complexes of **3** were crystallized by slow diffusion of methanol into a solution of the metalloporphyrin in dichloromethane, but these crystals were found to be twinned or of poor quality, and only the cell parameters could be

(27) Buchler, J. W.; Puppe, L. *Liebigs Ann. Chem.* **1974**, 1046.
(28) Dolphin, D. *J. Heterocycl. Chem.* **1970**, *7*, 275.
(29) Evans, B.; Smith, K. M.; Fuhrhop, J.-H. *Tetrahedron Lett.* **1977**, *5*, 443.
(30) van Geet, A. L. *Anal. Chem.* **1970**, *42*, 679.

Table I. Crystal Structure Data for Porphyrin **3** and Selected Calculated Structural Parameters for Ni**3**

	NH (N21/N23)	no NH (N22)	av **3**	calcd Ni**3**
		Displacements[a]		
N	0.14	0.01	0.08	0.00
C_a	0.34	0.39	0.37	0.27
C_b	0.78	1.20	0.99	1.05
C_m			0.00	0.02
		Planes		
pyrrole planarity (Å)[b]	<0.02	<0.03		*c*
pyrrole tilting (deg)[d]	18.0	33.6	25.8	26.1
pyrrole phenyl twist[e]	62.6	66.1	64.4	62.2
meso phenyl twist[f]			43.8	42.0
		Bond Length[g]		
$N-C_a$	1.366 (7)	1.366 (8)	1.366	
C_a-C_b	1.449 (10)	1.464 (9)	1.457	
C_b-C_b	1.405 (14)	1.368 (10)	1.387	
C_a-C_m	1.414 (8)	1.410 (9)	1.412	
C_b-C_{ph}	1.488 (9)	1.486 (9)	1.487	
C_m-C_{ph}			1.496 (9)	
		Bond Angles[g]		
$N-C_a-C_b$	106.7 (5)	110.7 (5)	108.7	
$N-C_a-C_m$	122.6 (6)	125.5 (6)	124.1	
C_a-N-C_a	112.1 (7)	105.9 (5)	109.0	
$C_a-C_b-C_b$	107.3 (3)	106.2 (6)	106.8	
$C_m-C_a-C_b$	130.5 (6)	123.7 (6)	127.1	
$C_a-C_m-C_a$			123.0 (6)	
$C_a-C_b-C_{ph}$	127.3 (6)	125.3 (6)	126.3	
$C_b-C_b-C_{ph}$	125.3 (4)	126.7 (6)	126.0	
$C_a-C_m-C_{ph}$	120.6 (6)	116.4 (6)	118.5	

[a] From the least-squares plane of the meso carbon atoms. [b] Largest deviation of any atom in a pyrrole ring from the least-squares plane of the pyrrole ring. [c] All torsion angles in the pyrrole rings <5°. [d] Mean angle between the least-squares plane of a pyrrole ring and the least-squares plane of the meso carbon atoms. [e] Mean angle between the least-squares planes of the phenyl and pyrrole rings. [f] Mean angle between the least-squares plane of a meso phenyl ring and the least-squares plane of the meso carbon atoms. [g] Average bond length or bond angle. Figures in parentheses are estimated standard deviations for individual bond lengths or angles within a molecule.

Table II. Crystal Structure Data and Calculated Structural Parameters for Ni**4c**

	Ni**4c**	calcd Ni**4c**	ruffled NiOEP[37]	planar NiOEP[38]
		Displacements[a]		
Ni	0.04	0.07	0.00	<0.01
N	0.02	0.01	<0.01	<0.01
C_a	0.46	0.40	0.30	<0.05
C_b	0.30	0.25	0.21	<0.08
C_m	0.83	0.78	0.51	<0.04
		Planes		
pyrrole twist[b]	25.1	20.7	14.2	*c*
pyrrole[d] planarity	<0.02	*e*	<0.02	<0.01
		Bond Lengths[f]		
Ni-N	1.911 (8)	1.911	1.929 (3)	1.958 (2)
$N-C_a$	1.384 (13)	1.400	1.386 (2)	1.376 (6)
C_a-C_b	1.442 (14)	1.435	1.449 (5)	1.443 (3)
C_a-C_m	1.402 (14)	1.388	1.372 (1)	1.371 (4)
C_b-C_b	1.345 (15)	1.297	1.362 (5)	1.346 (2)
C_b-CH_2	1.509 (14)	1.454	1.501	1.495
CH_2-CH_n	1.533 (15)	1.526	1.536	1.522
C_m-CH_2	1.501 (15)			
		Bond Angles[f]		
N-Ni-N	90.0 (3)	89.9	90.0	90.15 (9)
$Ni-N-C_a$	126.6 (7)	126.5	127.4 (2)	128.0 (2)
$N-C_a-C_m$	124.5 (9)	125.3	124.0 (2)	124.4 (3)
$N-C_a-C_b$	108.9 (8)	107.1	110.6 (2)	111.6 (3)
C_a-N-C_a	106.8 (8)	107.0	105.1 (3)	103.9 (4)
$C_a-C_m-C_a$	120.7 (9)	118.8	124.1 (2)	125.1 (2)
$C_a-C_b-C_b$	107.6 (9)	109.3	106.8 (3)	106.5 (4)
$C_m-C_a-C_b$	124.5 (9)	127.5	124.0 (2)	124.4 (3)
$C_a-C_b-CH_2$	139.7 (9)	136.6	124.9	125.5
$C_b-C_b-CH_2$	112.4 (9)	114.0	128.2	128.0
$C_b-CH_2-CH_n$	102.5 (8)	101.4	112.8	113.5
$CH_2-CH_2-CH_2$	108.8 (9)	108.7		

[a] From N4 or NiN4 least-squares plane. [b] Mean angle between least-squares plane of pyrrole ring and N4 or NiN4 least-squares plane. [c] Essentially planar (2.1° between planes of adjacent pyrrole rings). [d] Largest deviation of any atom in a pyrrole ring from the least-squares plane of the pyrrole ring. [e] All torsion angles in the pyrrole rings <5°. [f] Average bond length or bond angle. Figures in parentheses are estimated standard deviations for individual bond lengths or angles within a molecule.

obtained. Two crystalline forms of Co**3** were obtained: (1) blue plates, tetragonal, $a = b = 23.872$ (11) Å, $c = 8.389$ (5) Å, $V = 4780$ (5) Å^3, $Z = 2$; and (2) parallelepipeds, triclinic, $a = 15.055$ (9) Å, $b = 15.392$ (7) Å, $c = 32.32$ (1) Å, $\alpha = 93.25$ (4)°, $\beta = 98.035$ (46)°, $\gamma = 89.988$ (43)°, $V = 7403$ (7) Å^3, $Z = 4$. One crystalline form of Cu**3** was found: triclinic, $a = 15.111$ (19) Å, $b = 15.553$ (17) Å, $c = 32.467$ (47) Å, $\alpha = 93.31$ (10)°, $\beta = 98.31$ (11)°, $\gamma = 89.79$ (9)°, $V = 7538$ (17) Å^3, $Z = 4$. Fortunately, free base **3** and Ni**4c** did afford crystals of a quality suitable for structure determinations.

Crystals of the free base form of **3** were prepared by slow diffusion of a 2% solution of KOH in ethanol into a solution of the porphyrin in dichloromethane. Dodecaphenylporphyrin is readily protonated by traces of acid or water, so alkaline conditions were necessary to avoid formation of the porphyrin dication during the crystallization process. The porphyrin crystallized with three methylene chlorides of solvation ($C_{92}H_{62}N_4 \cdot 3CH_2Cl_2$) in the orthorhombic space group $Cmc2_1$: red parallelepiped, 0.325 × 0.275 × 0.125 mm, $a = 31.025$ (15) Å, $b = 22.284$ (8) Å, $c = 11.182$ (5) Å, $V = 7731$ (6) Å^3, $Z = 4$. Data were collected at 130 K using the Wyckoff scan technique on a Siemens R3m/V diffractometer with graphite-monochromated Mo Kα radiation in the scan range $0 \le 2\theta \le 50°$. Two standard reflections were measured every 198 reflections and showed < 2% intensity change. Of the 6765 reflections collected ($0 \le h \le 38$, $0 \le k \le 27$, and $-13 \le l \le 0$) 4087 were unique and 2783 were considered observed with $F > 3.0\sigma(F)$. The data were corrected for Lorentz and polarization effects and also for absorption.[31] The structure was solved by random-start multisolution direct methods using the SHELXTL-PLUS software package.[32] This gave half of the molecule and the solvent molecules in the asymmetric unit. Hydrogen atoms were placed at calculated positions using a riding model with C–H = 0.96 Å and $U_{iso} = 0.04$. The final cycle of refinement included 501 variable parameters and converged with $R = 0.063$ and $R_w = 0.065$. A triclinic modification of **3** was also obtained from the same crystallization tube. The crystals of this modification were twinned and/or of bad quality, and this permitted no data collection. The cell parameters were determined: $a = 16.271$ (3) Å, $b = 16.530$ (4) Å, $c = 18.333$ (6) Å, $\alpha = 72.09$ (2)°, $\beta = 83.20$ (2)°, $\gamma = 65.54$ (2)°, $V = 4269$ (2) Å^3, $Z = 2$.

Crystals of Ni**4c** were prepared by slow diffusion of methanol into a solution of the porphyrin in dichloromethane. The crystals were obtained as red parallelepipeds (0.8 × 0.2 × 0.2 mm) in the triclinic space group $P\bar{1}$ with one molecule of methylene chloride solvent ($C_{52}H_{68}N_4Ni \cdot CH_2Cl_2$): $a = 13.010$ (7) Å, $b = 13.166$ (4) Å, $c = 14.686$ (8) Å, $\alpha = 109.76$ (3)°, $\beta = 98.21$ (4)°, $\gamma = 94.11$ (3)°, $V = 2323$ (2) Å^3, $Z = 2$. Data were collected at 130 K with graphite-monochromated Mo Kα radiation in the scan range $0° \le 2\theta \le 45°$. Of the 6385 reflections collected, 6068 were unique, and of those, 3364 were considered observed with $F > 3.0\sigma(F)$. Standard Lorentz, polarization, and absorption corrections were applied,[31] and the structure was solved by direct methods.[32] Some atoms of the pentyl side chains (C155, C202, and C203) were refined as disordered over two positions with occupancies of 0.6 and 0.4 for all three atoms. The chlorine atoms of the solvent molecule were refined as disordered over two (occupancy 0.8:0.2) and three (0.33 each) positions. Hydrogens (except for those of the solvent molecule) were placed at calculated positions using the same riding model mentioned above. Anisotropic refinement for all non-hydrogen atoms, excluding the disordered atoms, yielded $R = 0.080$ and $R_w = 0.091$. A second crystalline modification was obtained from the same crystallization tube as red plates. The structure of this modification could not be determined due to poor crystal quality. Cell parameters: orthorhombic lattice, $a = 18.282$ (23) Å, $b = 18.881$ (17) Å, $c = 26.454$ (16) Å, $V = 9100$ Å^3, $Z = 8$.

Molecular Mechanics Calculations. Molecular mechanics calculations using BIOGRAF software (Polygen/Molecular Simulations) were carried out and displayed on a Silicon Graphics 4D210 Power Series

(31) Hope, H.; Moezzi, B. XABS. University of California, Davis, **1987**. The program obtains an absorption tensor from $F_o - F_c$ differences.

(32) Sheldrick, G. M. SHELXTL-PLUS. Program for crystal structure solution. Universität Göttingen, Germany, **1989**.

Table III. Calculated Minimum Energies (kcal mol^{-1}) and Selected Structural Parameters Obtained from Molecular Mechanics Calculations for Ni3, Ni4a–c, and Ni5

porphyrin		total[a]	bond	angle	torsion	van der Waals	M–N (Å)	N–M–N (deg)	C_a–N–N–C_a (deg)
Ni3[b]		535.5	28.9	82.8	279.6	139.5	1.915	163.8	1.7
Ni4c	*aaae*	269.4	16.7	152.4	46.9	51.6	1.911	175.5	41.5
Ni4a		226.1	11.9	144.1	38.2	30.4	1.913	180.0	38.9
Ni4b	*aaaa*	248.2	13.3	149.8	48.3	35.5	1.900	178.9	44.7
Ni4b	*aaae*	248.5	13.4	150.0	48.5	35.3	1.905	178.2	43.2
Ni4b	*aeae*	248.6	13.5	150.1	48.8	35.1	1.909	176.7	41.7
Ni4b	*aaee*	249.1	13.6	150.2	48.6	35.5	1.909	179.4	41.3
Ni4b	*aeee*	249.6	13.9	150.3	48.5	35.8	1.915	178.3	39.4
Ni4b	*eeee*	250.6	14.5	150.5	48.0	36.9	1.921	180.0	36.9
Ni5	*aaaa*	239.2	15.3	87.3	69.5	66.3	1.882	178.9	50.3
Ni5	*aaae*	242.9	15.5	89.0	70.7	66.9	1.889	177.3	48.8
Ni5	*aeae*	247.2	15.8	91.0	71.8	67.8	1.897	174.7	47.1
Ni5	*aaee*	248.6	15.8	91.2	72.2	68.4	1.895	179.7	47.0
Ni5	*aeee*	254.9	16.6	94.7	72.1	70.4	1.887	177.4	51.5
Ni5	*eeee*	262.1	17.4	98.5	72.6	72.4	1.878	179.9	55.7

[a] A small inversion term (<5 kcal mol^{-1}) is not listed but is included in the total energy. [b] Taken from ref 12.

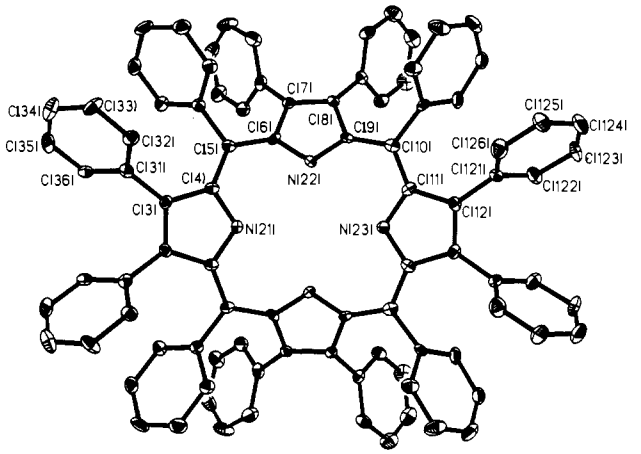

Figure 3. Molecular structure and labeling scheme for porphyrin **3**. The ellipsoids show 50% occupancy.

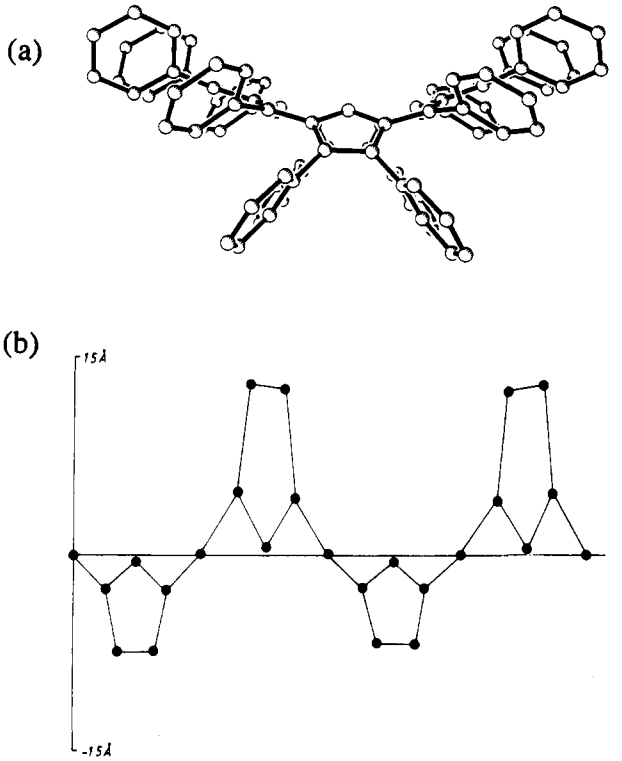

Figure 4. (a) Plots generated from the crystal structure of porphyrin **3** showing a saddle conformation of the macrocycle. The pyrrole rings are tilted alternately up or down with respect to the least-squares plane of the 24 atoms of the porphyrin core. (b) Linear display of the deviations of the macrocycle atoms from the least-squares plane of the meso carbon atoms.

workstation. The nickel(II) porphyrin force field used for the calculations has been described previously.[12] It is based on the normal coordinate analysis of NiOEP[33] and the Dreiding II forcefield.[34] The total calculated energies include contributions from bond stretching and bending, torsions, inversions (improper torsions), and van der Waals energies.

The energy minimization procedure utilized a conjugate-gradient technique. Planar, ruffled, and saddle conformations were generally used as starting points in the minimization procedure, with the aim of avoiding local energy minima. For the initial planar structures, the alkyl chains and phenyl rings were defined as orthogonal to the plane of the macrocycle and the alkyl chains of **4c** were set to all-trans conformations. The initial minimum energy structures were subjected to molecular dynamics simulations and then energy minimized again. This procedure was repeated until the total calculated energy did not change between minimizations.

Minimum energy structures were calculated for Ni**4a**, Ni**4b**, Ni**4c**, and Ni**5**. Minimum energy structures were also calculated for the zinc(II) complexes of **3** and **4c** to determine if the porphyrin conformations were metal-dependent. The zinc porphyrin force field was obtained by modifying the metal parameters and leaving the remainder of the force field unchanged. The new parameters for zinc were R_{eq} = 2.145 Å, R_{nb} = 4.54 Å, and atomic mass = 65.380. Full details of the parameters for other metals are presented elsewhere.[35]

For porphyrin **3** a structure was calculated using standard Dreiding II parameters to represent the inner hydrogen atoms. Unfortunately, the resulting structure was unrealistic and gave angles between the meso phenyl and porphyrin planes as low as 19°. Ni**3** was therefore used for comparison purposes. This is probably a reasonable approximation to the free base porphyrin as the macrocycle conformation should largely be controlled by the peripheral substituents. For example, porphyrin **1b** adopts essentially the same nonplanar structure for the free base, dication, Ni(II), Co(II), Cu(II), and Zn(II) complexes, with only small changes in the out-of-plane displacements.[9,15a,35] Energies and selected structural parameters obtained from the molecular mechanics calculations are given in Tables I–III.

Results and Discussion

Crystal Structures. The molecular structure and numbering scheme for porphyrin **3** is shown in Figure 3. An edge-on view of the macrocycle (Figure 4) shows that the porphyrin pyrrole rings are alternately tilted up and down with respect to the least-squares plane of the 24 atoms of the porphyrin core, i.e., the macrocycle is distorted into a very nonplanar saddle conformation.[2]

(33) (a) Abe, M.; Kitagawa, T.; Kyogoku, Y. *J. Chem. Phys.* **1978**, *69*, 4526. (b) Li, X.-Y.; Czernuszewicz, R. S.; Kincaid, J. R.; Spiro, T. G. *J. Am. Chem. Soc.* **1989**, *111*, 7012. (c) Li, X.-Y.; Czernuszewicz, R. S.; Kincaid, J. R.; Stein, P.; Spiro, T. G. *J. Chem. Phys.* **1990**, *94*, 47.

(34) Mayo, S. L.; Olafson, B. D.; Goddard, W. A. *J. Phys. Chem.* **1990**, *94*, 88.

(35) Sparks, L. D.; Medforth, C. J.; Park, M.-S.; Chamberlain, J. R.; Ondrias, M. R.; Senge, M. O.; Smith, K. M.; Shelnutt, J. A. *J. Am. Chem. Soc.*, in press.

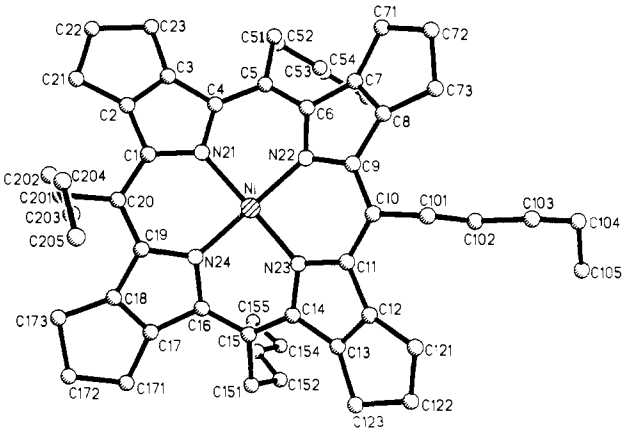

Figure 5. Molecular structure and labeling scheme for porphyrin Ni**4c**.

This saddle distortion is not as symmetrical as the distortions seen for other saddle-shaped dodecasubstituted metalloporphyrins.[9,12,15a,35] The angles between the least-squares planes of the pyrrole rings and the least-squares plane of the meso carbon atoms are 33.6° for the pyrrole ring without a hydrogen (N22) but only 18.0° for the pyrrole rings with hydrogens (N21 and N23).

The crystal structure of porphyrin **3** was examined for any intermolecular contacts which could be responsible for the observed nonplanar conformation. Generally, the intermolecular contacts were greater than 4 Å. This indicates that the observed nonplanarity does not arise from crystal packing forces but from a minimization of steric repulsions between the peripheral phenyl rings. The nonplanar conformation of the macrocycle and the tilting of the phenyl rings into the porphyrin plane effectively minimize unfavorable contacts between the peripheral substituents. Contacts between meso and pyrrole phenyl ipso carbons vary between 2.99 and 3.12 Å, and those between pyrrole phenyl ipso carbons and the meso ortho carbons range from 3.01 to 3.91 Å.

The structural parameters for **3**, including bond lengths and angles, are summarized in Table I. In general, the bond length and bond angle differences for pyrrole rings with and without hydrogens are similar to those seen for planar triclinic TPP.[36]

The molecular structure and numbering scheme for Ni**4c** is shown in Figure 5. An edge-on view of the macrocycle (Figure 6) shows that in this case alternate pyrrole rings are twisted clockwise or counterclockwise about the Ni–N bond such that the meso carbons are alternately above or below the least-squares plane of the 24 atoms of the porphyrin core. Ni**4c** therefore adopts a ruffled conformation.[2] The absence of any appreciable intermolecular contacts less than 4 Å which could be responsible for the observed nonplanarity suggests that the conformation of Ni**4c** is also due to the substituents and is not the result of crystal packing forces.

Structural parameters for Ni**4c**, and for comparison those of ruffled (tetragonal) NiOEP[37] and planar (triclinic A) NiOEP,[38] are summarized in Table II. Ni**4c** is clearly much more ruffled than the tetragonal form of NiOEP.[37] This is to be expected if the nonplanarity of Ni**4c** is due to the peripheral substituents. Ni**4c** shows a decrease in both the Ni–N distance and the C_a–C_m–C_a angle as the core contracts and the porphyrin becomes more nonplanar than ruffled NiOEP.

The conformations seen for the pentyl substituents of Ni**4c** are quite interesting. The chains at C5, C15, and C20 have the corresponding β-methylene carbons (C52, C152, and C202) displaced away from the mean plane of the macrocycle in quasi-axial orientations (designated "*a*"), whereas the pentyl chain at C10 has C102 folded back toward the plane in a quasi-equatorial environment (designated "*e*"). The presence of *a* and *e* alkyl groups in solution (as determined by low-temperature NMR spectroscopy, see below) shows that this effect is not the result of crystal packing forces. Moreover, the NMR results show that the *aaae* conformation of Ni**4c** observed in the crystalline state is also the dominant conformation in solution.

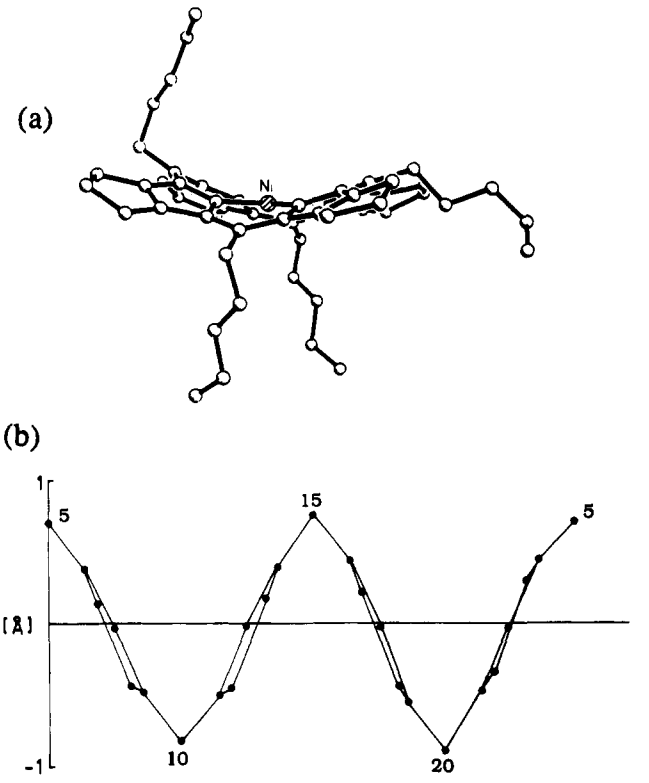

Figure 6. (a) Plots generated from the crystal structure of Ni**4c** showing a ruffled conformation of the macrocycle. Alternate pyrrole rings are twisted clockwise or counterclockwise about the Ni–N bond such that the meso carbons are alternately above or below the least-squares plane of the 24 atoms of the porphyrin core. (b) Linear display of the deviations of the macrocycle atoms from the least-squares plane of the nitrogen atoms.

Differences between the *a* and *e* orientations were examined. C102 is only 0.19 Å out of the least-squares plane defined by the four nitrogen atoms, compared with displacements of 2.79 Å for C52, 2.91 Å for C152, and 3.10 Å for C202. For the groups in axial conformations the closest contacts (in Å) are C52–C4, 3.22; C152–C14, 3.19; and C202–C1, 3.22. For the C102 group in an equatorial conformation the closest contacts (in Å) are slightly larger: 3.33 (C11) and 3.33 (C9).

Some of the pentyl chains are also disordered in the crystal structure. Starting from the porphyrin and working outward, the C20 chains is in gauche–trans–trans and gauche–trans–gauche conformations. The βCH_2–αCH_2–C_m–C_a torsion angles are not equivalent for these two chains and show that the gauche–trans–trans chain is tilted toward C21 and the gauche–trans–gauche chain is tilted toward C173. The other disordered chain is at C15, which has the terminal methyl group in two different locations. This gives gauche–trans–gauche and gauche–trans–trans conformations, both of which tilt toward C123. The C5 chain is in a single gauche–trans–trans conformation and tilts toward C23. The equatorial C10 chain is in a single trans–trans–gauche conformation and has βCH_2–αCH_2–C_m–C_a torsion angles of approximately 90°. Clearly, crystal packing forces must to some extent control the conformations of the pentyl chains as the chains do not adopt the extended all-trans conformation that might be expected to predominate in solution.

Molecular Mechanics Calculations. The minimum energy structure for Ni**3** is calculated to be a saddle conformation (Figure 7), which is the same distortion mode seen in the crystal structure of the free base porphyrin (Figure 4). The agreement between the observed and calculated values for the out-of-plane displacements, pyrrole tilt angles, and phenyl twist angles is generally

(36) Silvers, S. J.; Tulinsky, A. *J. Am. Chem. Soc.* **1967**, *89*, 3331.
(37) Meyer, E. F. *Acta Crystallogr.* **1972**, *B28*, 2162.
(38) Cullen, D. L.; Meyer, E. F. *J. Am. Chem. Soc.* **1974**, *96*, 2095.

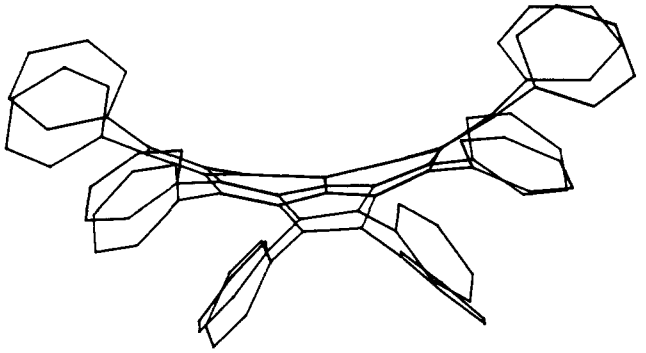

Figure 7. Calculated minimum energy structure for Ni3.

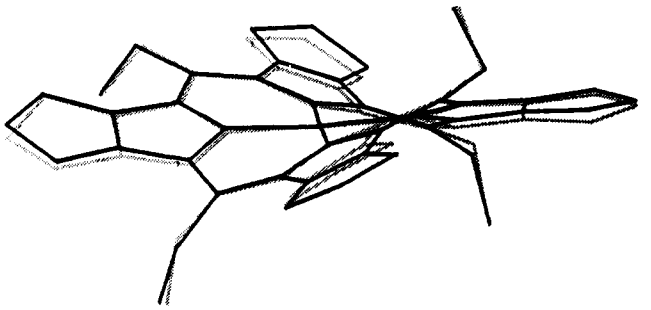

Figure 8. Calculated minimum energy structure (solid lines) and crystal structure (gray lines) for Ni**4c**. The last three carbon atoms of each pentyl chain have been omitted. For the 24 porphyrin core atoms the root mean square deviation between the observed and calculated structures is 0.08 Å.

quite good (Table I). This probably reflects the fact that the nitrogen substituents have only a small effect on the structure, i.e., the nonplanarity is primarily due to the peripheral substituents. As noted earlier, porphyrin **1b** adopts essentially the same nonplanar saddle structure for the free base, dication, Ni(II), Co(II), Cu(II), and Zn(II) complexes, with only small changes in the out-of-plane displacements.[9,15a,35] The Ni–N distance calculated for Ni3 (1.915 Å) is also in excellent agreement with the Ni–N distance determined by EXAFS using a powder sample (1.92 ± 0.02 Å).[15a]

The similarity of the observed and calculated structures for **3** further confirms that the saddle distortion is due to the steric repulsion that exists between the peripheral substituents. An attempt was therefore made to estimate the energy difference between planar and nonplanar conformations of Ni3. The energy of a relaxed planar structure was estimated by stopping the energy minimization of a planar structure just before the macrocycle began to distort into a nonplanar conformation. The relaxed planar structure is approximately 25 kcal mol^{-1} higher in energy than the calculated minimum energy saddle structure. Other nonplanar conformations with varying degrees of pyrrole twisting and tilting were much closer in energy to the minimum energy structure. The second crystalline form of **3** could be in one of these other nonplanar conformations, or alternatively it could arise from a different packing arrangement of the same macrocycle conformation shown in Figure 4.

For the *aaae* isomer of Ni**4c** a direct comparison between the observed and calculated structures was possible, and the matched structures are shown in Figure 8. The last three carbon atoms of each pentyl chain were omitted because the positions of these carbons are influenced by packing forces in the crystal. For the 24 core atoms the root mean square deviation between the observed and calculated structures was 0.08 Å, which is approximately the same error obtained when crystal structures of Co, Cu, and Zn complexes of porphyrin **1b** were matched to calculated structures.[35]

The structural parameters calculated for Ni**4c** generally agree well with the crystallographic data (Table II). The bond distances are generally reproduced to within 0.02 Å and the bond angles to within 2°, roughly the same errors noted for the observed and calculated structures of NiOEP in the original parameterization.[12] The differences between the observed and calculated structures occur primarily for the propano ring, where the calculated C_b–C_b and C_b–CH_2 bond lengths are about 0.05 Å shorter than in the crystal structure, and the C_a–C_b–CH_2 angle is about 3° smaller than the crystal structure value. Small errors of this type are not unreasonable given that a generic force field was used in the calculations.

The energy of a planar conformation for Ni**4c** was estimated using the same procedure described for Ni3, although Ni**4a** was used to avoid having to consider the *a* and *e* conformations of the alkyl chains. A planar species was calculated to be approximately 24 kcal mol^{-1} higher in energy than the minimum energy ruffled form of Ni**4a**.

The energies for Ni**4b** with different *a* and *e* orientations of the ethyl groups were calculated to differ by less than 2.5 kcal mol^{-1} (Table III), thereby providing one possible explanation for the second crystalline form of Ni**4c**. A larger number of *e* groups causes an increase in the total calculated energy of the structure and gives rise to a less ruffled conformation (as evidenced by a decrease in the C_a–N–N–C_a torsion angle). The relative energies calculated for the Ni**4b** structures are in qualitative agreement with those determined experimentally by variable temperature NMR spectroscopy (see below).

The minimum energy structures calculated for Zn3 and Zn**4c** (not shown) are slightly more planar than the corresponding nickel(II) porphyrins but retain the same general distortion mode. An increase in planarity for the zinc(II) porphyrins is reasonable because the small nickel(II) atom is believed to favor a more nonplanar conformation of the porphyrin macrocycle in order to obtain a shorter metal to nitrogen distance.[1] Details of calculations describing the effects of a range of metal ions on the planarity of porphyrin **1b** are described elsewhere.[35]

Finally, energies were calculated for Ni**5** with all different *a* and *e* orientations of the ethyl groups (Table III). The aim of these calculations was to evaluate any increase in peripheral steric strain which could explain why dihydroporphyrin **6** was obtained from the synthesis rather than porphyrin **5**. The orientation of the ethyl groups does have a much larger effect on the total energy calculated for Ni**5** (E_{eeee}–E_{aaaa} = 22.9 kcal mol^{-1}) than it does for Ni**4b** (E_{eeee}–E_{aaaa} = 2.4 kcal mol^{-1}), presumably because of increased peripheral steric crowding for the six- vs five-membered rings. In agreement with this observation, Ni**5** is also calculated to be more nonplanar than Ni**4b**, as evidenced by an increase in the C_a–N–N–C_a torsion angle and a shorter Ni–N bond distance.

Comparisons with Structures of Other Nickel(II) Porphyrins. Crystal structures for nickel(II) complexes of **1b**, **1c**, **2b**, and **2c** show a very nonplanar saddle conformation of the porphyrin macrocycle,[15a] and similar saddle structures are calculated as minimum energy structures for these porphyrins.[12] The crystal structure of **3** also shows a saddle conformation (except that the opposite pairs of pyrrole rings tilt by very different amounts), and a saddle conformation is the minimum energy structure calculated for Ni3. The crystal structure of Ni**4c** and the minimum energy structures calculated for Ni**4a–c** all show a ruffled conformation.

These observations imply that meso phenyl groups favor a saddle conformation and meso alkyl groups favor a ruffled conformation for the dodecasubstituted nickel porphyrins. Molecular modeling studies indicate that the hydrogens on the first carbon atom of a meso alkyl group force the alkyl group out of plane, thus moving the meso carbon atom out of plane and giving rise to a ruffled conformation.

Variable Temperature NMR Studies.

Recent studies[9,11,16] have demonstrated that in some cases variable temperature NMR spectroscopy can be used to show that dodecasubstituted porphyrins adopt nonplanar conformations in solution. We have carried out a thorough investigation of the temperature dependence of the NMR spectra of **3** and **4a–c** with the aim of obtaining information about the conformations of these porphyrins in solution.

The 500-MHz proton NMR spectrum of **3** as a function of temperature is shown in Figure 9. The spectrum at 193 K shows

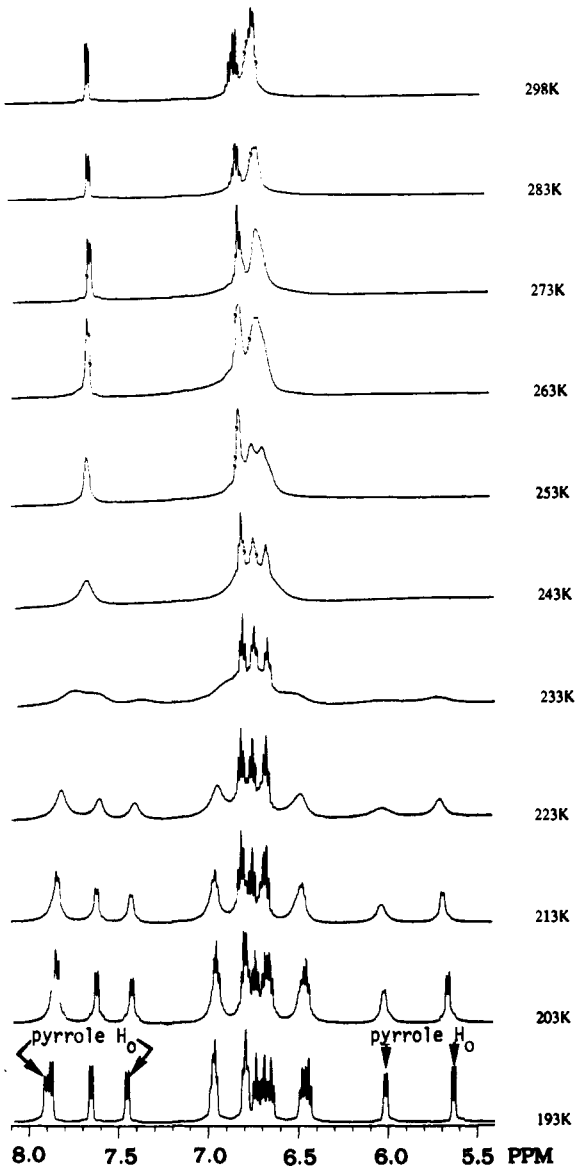

Figure 9. Temperature dependence of the 500-MHz proton NMR spectrum of **3** in CD_2Cl_2.

six doublets and nine triplets, whereas the spectrum at 298 K overlaps somewhat but appears to show three signals each for the meso and pyrrole phenyl rings. Coalescence occurs between 253 and 263 K for two triplets and between 233 and 243 K for the downfield doublet. The chemical shift differences in the slow-exchange spectra are sufficiently similar to preclude a single process from causing coalescence in both cases.

The unusually wide range of chemical shifts seen for the ortho protons of the pyrrole phenyl rings in the free base and dication at low temperatures (Figures 9 and 10) must be due to the ring current of the porphyrin macrocycle. The ortho protons which point back into the saddle-shaped porphyrin core are expected to be shielded compared to the protons which point down into the plane. The chemical shift differences between pyrrole ortho protons are similar for both the free base and dication, implying similar conformations.

Porphyrin **3** must undergo two dynamic processes. One dynamic process for **3** was identified as NH tautomerism.[39,40] The value of ΔG^* calculated[39] for this process (13.0 kcal mol^{-1}) is comparable to that measured for TPP.[40] By analogy with related

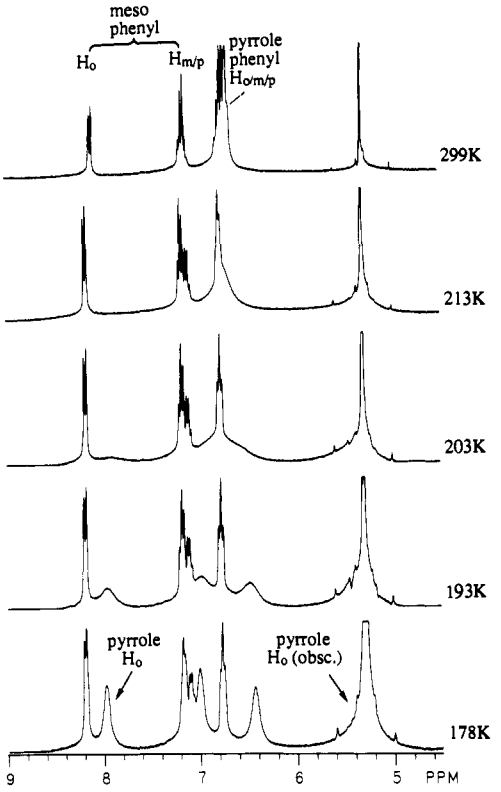

Figure 10. Temperature dependence of the 300-MHz proton NMR spectrum of the dication of **3** in CD_2Cl_2 plus 1% trifluoroacetic acid.

nonplanar porphyrins,[9,11] the second dynamic process for **3** (ΔG^* = 10.9–11.3 kcal mol^{-1}) was assigned as inversion of the saddle-shaped porphyrin macrocycle as shown in Figure 11.

For the dication ($H_4\mathbf{3}^{2+}$) only one dynamic process was observed (Figure 10). $H_4\mathbf{3}^{2+}$ is almost certainly in a saddle conformation similar to that seen in the crystal structures of the TPP dication[41] and free base **3**, so the single dynamic process was also assigned as macrocyclic inversion. The standard equation gave ΔG^* as 10.9 kcal mol^{-1}.

No dynamic process was observed for Ni**3** ($\Delta G^* < 7.0$ kcal mol^{-1}), although this porphyrin must also be nonplanar. Presumably, the macrocyclic inversion barrier for Ni**3** is too low to be detected. This agrees with data for **1b**, **2b**, and **2c** which indicates that the nickel complexes have lower barriers to macrocyclic inversion than free base porphyrins or dications.[11] For example, Ni**2b** is calculated to adopt a very nonplanar saddle conformation[11,12] and its crystal structure shows a similar conformation of the macrocycle.[15a] However, macrocyclic inversion cannot be frozen out for Ni**2b**.

NMR studies gave considerably more information about the solution conformations of the dodecaalkylporphyrins **4a–c**. The signals for the propano protons provide a way to differentiate the saddle and ruffled distortion modes. By analogy with the TPP dication[41] the dications of porphyrins **4a–c** are expected to adopt saddle conformations. In this case both the α- and β-methylene protons should be diastereotopic when macrocyclic inversion is slow on the NMR time scale. The crystal structure of Ni**4c** and the molecular mechanics calculations for Ni**4a–c** show that these porphyrins adopt ruffled conformations. If the porphyrin were to distort by twisting of the pyrrole rings to give an idealized ruffled conformation, only the α-methylene protons should be diastereotopic. The β-methylene protons would not be diastereotopic because the β-methylene carbon is on the axis of rotation for the pyrrole ring. Diastereotopicity of the β-methylene protons would be dependent upon the orientations of the meso alkyl groups. If the nonplanarity involved both distortion modes, then both the α-methylene and β-methylene protons would be diastereotopic.

(39) Abraham, R. J.; Fisher, J.; Loftus, P. *Introduction to NMR spectroscopy*; Wiley: Chichester, **1988**.
(40) Abraham, R. J.; Hawkes, G. E.; Smith, K. M. *Tetrahedron Lett.* **1974**, *16*, 1483.
(41) Stone, A.; Fleischer, E. B. *J. Am. Chem. Soc.* **1968**, *90*, 2735.

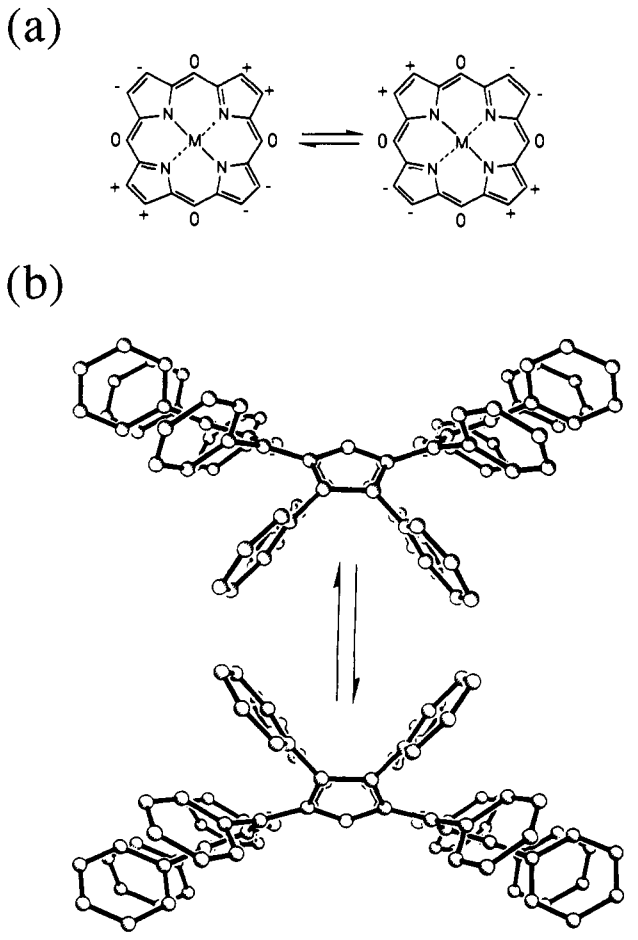

Figure 11. Representations of the macrocyclic inversion process for the saddle structure of porphyrin **3**. (a) Displacements of the atoms with respect to the porphyrin least-squares plane are shown as + = above the plane, − = below the plane, and 0 = in the plane. (b) The inversion process approximated using figures generated from the crystal structure of **3**.

The 300-MHz proton NMR spectrum of the dication of **4b** (H_4**4b**$^{2+}$) as a function of temperature is shown in Figure 12. Upon cooling, both the α- and β-methylene protons become diastereotopic, in agreement with the porphyrin adopting a saddle conformation. The activation energies for macrocyclic inversion increase as the chain becomes progressively longer: ΔG^* (kcal mol^{-1}) H_4**4a**$^{2+}$, 9.2–9.3; H_4**4b**$^{2+}$, 11.7–11.8; and H_4**4c**$^{2+}$, 11.9–12.1. H_4**4b**$^{2+}$ and H_4**4c**$^{2+}$ also showed a second dynamic process, with ΔG^* = 9.3 and 10.3 kcal mol^{-1}, respectively. This process was assigned to rotation of the alkyl group about the C_{meso}–CH_2 bond.

A variable temperature NMR study for Ni**4b** is shown in Figure 13. The proton spectrum at 174 K is consistent with a ruffled conformation of the macrocycle as only the α-methylene protons are diastereotopic (a representation of the macrocyclic inversion process required to average the α-methylene proton chemical shifts is shown in Figure 15). Activation energies for macrocyclic inversion again increased as the meso alkyl chain became longer: ΔG^* (kcal mol^{-1}) Ni**4a** < 8.0; Ni**4b**, 11.2; and Ni**4c**, 12.5.

The methyl region from the spectrum of Ni**4b** at 174 K (Figure 14) shows one signal at 2.22 ppm, two signals at 1.56 ppm, and several signals at 0.85 ppm. Saturation transfer was observed at 193 K between the signals at 0.85 ppm and the signals at 1.56 and 2.22 ppm (spectra not shown). Decoupling the methylene signal at 4.26 ppm revealed that three signals were present in the group at 0.85 ppm (Figure 14).

The large chemical shift range of the methyl groups for Ni**4b** suggested the presence of *a* and *e* groups similar to those seen in the crystal structure of Ni**4c**. An *e* methyl group is predicted to be more in the plane of the porphyrin and deshielded compared to an *a* methyl group. On the basis of chemical shift considerations, integration ratios, and curve-fitting procedures, the most downfield signal (2.22 ppm, 1 H) was assigned as an *e* methyl group and the signals at 0.89 ppm (2 H) and 0.80 ppm (1 H) were assigned as *a* methyl groups in the *aaae* conformer. This is the

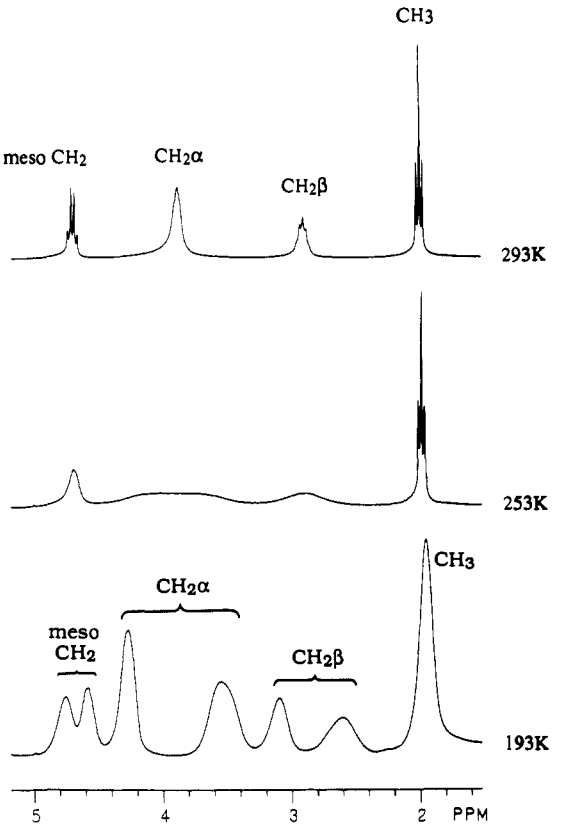

Figure 12. Temperature dependence of the 300-MHz proton NMR spectrum of the dication of porphyrin **4b** in CD_2Cl_2 plus 1% TFA.

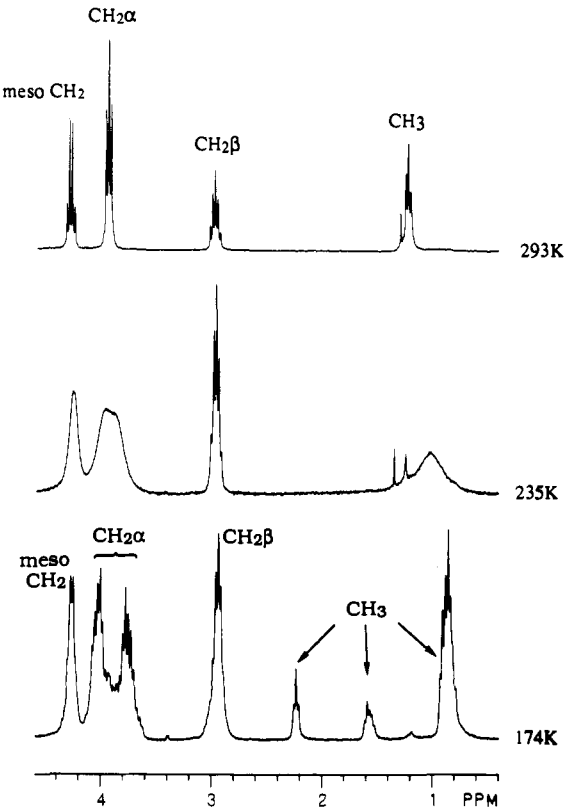

Figure 13. Temperature dependence of the 300-MHz proton NMR spectrum of Ni**4b** in CD_2Cl_2/CS_2 (1:3).

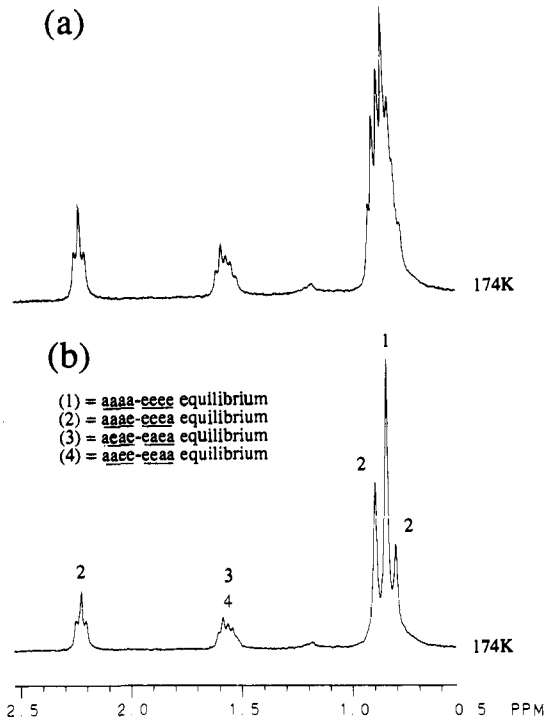

Figure 14. 300-MHz proton NMR spectrum of **Ni4b** at 174 K in CD_2Cl_2/CS_2 (1:3). (a) Expansion of the methyl region. (b) Expansion of the methyl region with the ethyl CH_2 at 4.26 ppm decoupled.

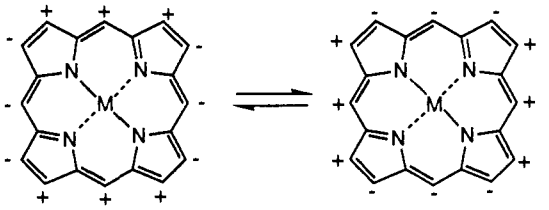

Figure 15. Representation of the macrocyclic inversion process for the ruffled conformations of **Ni4b** and **Ni4c**. Displacements of the atoms with respect to the porphyrin least-squares plane are shown as + = above the plane and − = below the plane.

same conformation seen in the crystal structure of **Ni4c**. The signal at 0.85 ppm (4 H) had a chemical shift very similar to the axial methyl groups and was assigned to the *aaaa* conformation.

To explain the remaining signals at 1.58 and 1.54 ppm, which are at approximately average values for *a* and *e* methyl groups,[42] a second dynamic process was invoked. In this process the relative orientations of the alkyl groups are retained and the *a* and *e* environments are exchanged, although it is not clear at this stage how this is achieved. Macrocyclic inversion with retention of relative ethyl configuration or correlated ethyl rotation are two possible mechanisms. With this additional process the spectrum of **Ni4b** at 174 K (Figure 14) can be rationalized in terms of four equilibria: (1) *aaaa* ⇔ *eeee*, (2) *aaae* ⇔ *eeea*, (3) *aeae* ⇔ *eaea*, and (4) *aaee* ⇔ *eeaa*. Equilibria 3 and 4 give averages of the chemical shifts for *a* and *e* methyl groups, thus explaining the signals at 1.58 and 1.54 ppm.

The energies calculated for different arrangements of the *a* and *e* groups in **Ni4b** (Table III) support this interpretation of the NMR data. Firstly, the calculated energy differences for the *aaaa* ⇔ *eeee* equilibrium (250.6 − 248.2 = 2.4 kcal mol^{-1}) and *aaae* ⇔ *eeea* equilibrium (249.6 − 248.5 = 1.1 kcal mol^{-1}) suggest that the *eeee* and *eeea* conformers should not be very highly populated. This explains why the observed spectra are more like those of the *aaaa* and *aaae* species. Secondly, equilibria 3 and 4 are calculated to be less populated than equilibria 1 and 2, and this agrees with the observed intensities.

The molecular mechanics calculations were done in the gas phase, so they cannot reproduce solvation effects. However, the NMR results obtained from the nonpolar CD_2Cl_2/CS_2 solvent system agree quite well with the calculated energies. With the caveat that the side chain conformations may be solvent-dependent, this result does lend further support to the use of molecular mechanics calculations in predicting porphyrin structures in solution.

The spectrum of **Ni4c** is complicated due to the methylene protons of the pentyl chains but is basically similar to that of **Ni4b**. Three signals are seen for the β-methylene protons of the pentyl groups when macrocyclic inversion is slow on the NMR time scale. The β-methylene proton signals at 2.57, 1.83, and 1.05 ppm presumably correspond to equatorial, time-averaged axial–equatorial, and axial environments. The intensities of these signals are approximately 1:1:5, giving the following composition for the conformational mixture: (1) *aaaa* ⇔ *eeee*, 29%; (2) *aaae* ⇔ *eeea*, 57%; and (3) *aeae* ⇔ *eaea* and (4) *aaee* ⇔ *eeaa*, 14% total. The conformation seen in the crystal structure of **Ni4c** therefore predominates in solution as well. For **Ni4b** the conformational mixture is slightly different: (1) *aaaa* ⇔ *eeee*, 44%; (2) *aaae* ⇔ *eeea*, 44%; and (3) *aeae* ⇔ *eaea* and (4) *aaee* ⇔ *eeaa*, 11% total.

Having successfully used variable temperature NMR experiments to determine the solution conformations of the dications and nickel complexes of porphyrins **4a–c**, we applied the same methodology to the free base dodecaalkylporphyrins. Porphyrin **4a** was not sufficiently soluble to be studied, but a dynamic process with an activation energy of approximately 13 kcal mol^{-1} was observed in the proton NMR spectra of **4b** and **4c**. Unfortunately, the proton spectra of **4b** and **4c** at low temperatures could not be readily interpreted in terms of ruffled or saddle conformations. A low temperature carbon-13 NMR study of porphyrin **4c** in CD_2Cl_2 indicated that the process observed was probably NH tautomerism.[39,40] At 294 K the carbon-13 spectrum of **4c** showed only one aromatic carbon (δ 117.6), whereas at 213 K a total of five carbons were seen (δ 152.8, 146.9, 144.9, 130.1, 117.1). The single signal seen at 294 K must be from the meso carbons, with the α- and β-pyrrole carbons being broadened beyond detection due to the NH tautomerism process. At 213 K two sets of signals were seen for α- and β-pyrrole carbons of pyrrole rings with and without hydrogens. The large chemical shift difference expected for the "pyrrole"- and "pyridine-like" α carbons[39] is clearly present.

Visible Absorption and Resonance Raman Spectra. Several recent studies have investigated the effects of nonplanarity on the visible absorption spectra of porphyrins.[8-12,43] These studies have shown that the optical spectra of nonplanar porphyrins are shifted to absorption at lower energy when compared to planar porphyrins. As the dodecaphenyl- and dodecaalkylporphyrins are known to adopt nonplanar conformations in solution, a similar effect should be seen in the visible absorption spectra of these porphyrins. Absorption maxima for **Ni3**, **Ni4a–c**, the essentially "planar" porphyrins NiTPP and **Ni2d**,[15b] and the very nonplanar saddle-shaped porphyrins **Ni2b** and **Ni2c**[15a] are summarized in Table IV. The optical data shows that the absorption maxima for **Ni3**

Table IV. Absorption Maxima for Nickel(II) Porphyrins in Dichloromethane

	λ_{max} (nm)		
porphyrin	γ	β	α
NiTPP[12]	414	525	557
Ni2d[15b]	408	522	554
Ni2b[12]	424	543	579
Ni2c[12]	440	556	595
Ni3	449	566	613
Ni4a	418	540	580
Ni4b	420	544	582
Ni4c	422	546	582

(42) A COSY spectrum at 178 K showed a similar average chemical shift for the methylene protons of the ethyl groups.

(43) Alden, R. G.; Crawford, B. A.; Doolen, R.; Ondrias, M. R.; Shelnutt, J. A. *J. Am. Chem. Soc.* **1989**, *111*, 2070.

and Ni**4a-c** are indeed shifted to lower energy compared to NiTPP and Ni**2d**, and that Ni**3** and Ni**4a-c** behave more like the very nonplanar porphyrins Ni**2b** and Ni**2c**. However, the magnitudes of the shifts in the absorption spectra of Ni**3** and Ni**4a-c** are quite different. This may be because the porphyrins are distorted from planarity in different ways and/or to different degrees. Alternatively, it may be because the porphyrins have substituents with different electron-donating characteristics. INDO/CI calculations show that the correct core conformation *and* substituents are necessary to reproduce the trends in optical spectra of Ni**1a**, Ni**1b**, Ni**2a**, and Ni**2b**.[35]

Raman spectra of Ni**3** and Ni**4a-c** also show quite clearly that these porphyrins exist in nonplanar conformations in solution. As Raman spectroscopy has previously been used to show that NiOEP is present as a mixture of both planar and nonplanar conformations in solution,[43] we attempted to determine if Ni**3** and Ni**4a-c** exist in multiple conformations in solution. Our results to date are inconclusive, but these studies are continuing.[44]

Conclusions

Dodecaphenylporphyrin (**3**) and the dodecaalkylporphyrins **4a-c** provide a unique opportunity to study many facets of porphyrin nonplanarity. We have investigated several aspects of the syntheses, structures, and spectroscopic properties of these porphyrins. Three of the key results obtained from our studies are as follows: (1) A very nonplanar saddle distortion is seen in the crystal structure of **3**, and a very nonplanar ruffled distortion is seen in the crystal structure of Ni**4c**. (2) These nonplanar distortions are correctly predicted by molecular mechanics calculations using a force field for nickel(II) porphyrins. (3) Variable temperature NMR studies indicate that the macrocycle conformations of **3** and Ni**4c** in solution are similar to those seen in the crystalline state.

Acknowledgment. Work performed at the University of California was supported by the National Science Foundation (CHE-90-01381, K.M.S.) and the Deutsche Forschungsgemeinschaft (Se 543/1-1, M.O.S.). Work performed at Sandia National Laboratories was supported by the U.S. Department of Energy (DE-AC04-76DP00789, J.A.S.). C.J.M. thanks the Fulbright Commission for the award of a travel scholarship. C.J.M. and L.D.S. thank the Associated Western Universities, Inc., for fellowships.

Supplementary Material Available: Details of the crystal structure determinations of **3** and Ni**4c** including lists of atomic coordinates, anisotropic thermal parameters, H-atom coordinates, bond lengths, bond angles, torsion angles, and least-squares planes (29 pages); observed and calculated structure factors for **3** and Ni**4c** (37 pages). Ordering information is given on any current masthead page.

(44) Sparks, L. D., Shelnuit, J. A.; Medforth, C. J.; Smith, K. M. Unpublished results.

Synthesis and Characterization of a Superoxo Complex of the Dicobalt Cofacial Diporphyrin $[(\mu\text{-}O_2)Co_2(DPB)(1,5\text{-diphenylimidazole})_2][PF_6]$, the Structure of the Parent Dicobalt Diporphyrin $Co_2(DPB)$, and a New Synthesis of the Free-Base Cofacial Diporphyrin $H_4(DPB)$

James P. Collman,*,† James E. Hutchison,† Michel Angel Lopez,‡ Alain Tabard,‡ Roger Guilard,‡ Won K. Seok,§ James A. Ibers,§ and Maurice L'Her⊥

Contribution from the Department of Chemistry, Stanford University, Stanford, California 94305, Université de Bourgogne, Laboratoire de Synthèse et d'Electrosynthèse Organométalliques associé au CNRS (URA 33), Faculté des Sciences "Gabriel", 21100 Dijon Cedex, France, Department of Chemistry, Northwestern University, Evanston, Illinois 60208-3113, and Université de Bretagne Occidentale URA CNRS 322, Faculté des Sciences, 6 Avenue Victor Le Gorgeu, 29287 Brest Cedex, France. *Received April 8, 1992*

Abstract: Chemical oxidation of the dicobalt cofacial diporphyrin $Co_2^{II/II}(DPB)$, followed by exposure to dioxygen affords the bridged superoxo complex $[(\mu\text{-}O_2)Co_2(DPB)][PF_6]$. This μ-superoxo complex has been implicated in possible mechanisms of four-electron dioxygen reduction by dicobalt cofacial diporphyrins but had not been isolated and fully-characterized previously. Although the superoxo complex is unstable with respect to loss of dioxygen, addition of 2 equiv of 1,5-diphenylimidazole yields $[(\mu\text{-}O_2)Co_2^{III/III}(DPB)(1,5\text{-diphenylimidazole})_2][PF_6]$, a μ-superoxo complex that is stable toward loss of dioxygen. Analytically pure samples of the latter complex have been prepared, and their spectral and electrochemical properties are described. The crystal structure of the parent dicobalt cofacial diporphyrin $Co_2^{II/II}(DPB)$ is reported. The Co–Co distance (3.726 (1) Å) and other structural features are compared to those of $Co_2(FTF4)$ and of other known metallo-DPB structures. A new, improved total synthesis of the free-base porphyrin $H_4(DPB)$ is presented. The combination of new reaction sequences, increased reaction scales, and improved product yields allows for large scale synthesis (gram quantities) of the free-base porphyrin needed to develop fully the coordination chemistry of the cofacial metallodiporphyrins.

The development of electrode materials that catalyze the four-electron reduction of dioxygen at or near the thermodynamic reduction potential (1.23 V vs NHE[1]) is important for fuel-cell technology and has been the subject of intense study. Although metallic platinum is an efficient fuel-cell cathode, its cost has prohibited routine use. Through the use of low loadings of platinum in solid polymer electrolytes, more economical, platinum-based fuel cells are presently being developed.[2] Still, there

† Stanford University.
‡ Université de Bourgogne.
§ Northwestern University.
⊥ Université de Bretagne Occidentale.

(1) Abbreviations: DPB^{4-} = diporphyrinato biphenylene tetraanion, DPA^{4-} = diporphyrinato anthracene tetraanion, DPIm = 1,5-diphenylimidazole, EPG = edge-plane graphite, $FeCp_2$ = ferrocene, NHE = normal hydrogen electrode, DMSO = dimethyl sulfoxide, THF = tetrahydrofuran.

0002-7863/92/1514-9869$03.00/0